Systematic analysis of cilia characteristics and Hedgehog signaling in five immortal cell lines

Arianna Gómez[1,2], Julie Craft Van De Weghe[1], Malaney Finn[1], and Dan Doherty[1*]

[1]Department of Pediatrics, University of Washington, Seattle, Washington, USA

[2]Molecular Medicine and Mechanisms of Disease PhD Program, Department of Laboratory Medicine and Pathology, University of Washington, Seattle, Washington, USA

*Corresponding author

E-mail: ddoher@uw.edu (DD)

Short title: Cilia characteristics and Hh signaling in immortal cell lines

Abstract

Dysfunction of the primary cilium, a microtubule-based signaling organelle, leads to genetic conditions called ciliopathies. Hedgehog (Hh) signaling is mediated by the primary cilium in vertebrates and is therefore implicated in ciliopathies; however, it is not clear which immortal cell lines are the most appropriate for modeling pathway response in human disease; therefore we systematically evaluated Hh in five commercially available, immortal mammalian cell lines: ARPE-19, HEK293T, hTERT RPE-1, NIH/3T3, and SH-SY5Y. All of the cell lines ciliated adequately for our subsequent experiments, except for SH-SY5Y which were excluded from further analysis. hTERT RPE-1 and NIH/3T3 cells relocalized Hh pathway components Smoothened (SMO) and GPR161 and upregulated Hh target genes in response to pathway stimulation. In contrast, pathway stimulation did not induce target gene expression in ARPE-19 and HEK293T cells, despite SMO and GPR161 relocalization. These data indicate that human hTERT RPE-1 cells and murine NIH/3T3 cells, but not ARPE-19 and HEK293T cells, are suitable for modeling the role of Hh signaling in ciliopathies.

Background

Primary cilia are microtubule-based organelles that transduce light, mechanical, and chemical signals into cells (1). Protruding from the surface of most cell types, primary cilia mediate multiple signaling pathways, including Hedgehog (Hh), that play important roles in development and tissue homeostasis. Cilium dysfunction results in conditions called ciliopathies, and while abnormal Hh signaling has been described in models of ciliopathy-associated genes, details of the disease mechanism have not been

43 clearly elucidated. (2). Immortal cell lines are frequently used to study primary cilium
44 biology and the mechanisms underlying ciliopathies (3–6); however, the strengths and
45 weaknesses of commonly used human cell lines have not been systematically
46 compared. The goal of this study was to identify immortal cell lines suitable for studying
47 Hh signaling in human health and disease.

48 In vertebrates, the primary cilium modulates the canonical Hh signaling pathway
49 through the coordinated translocation of Hh pathway proteins in and out of the cilium
50 (reviewed in (7)). In the absence of Hh ligand, ciliary localization of the Patched (PTCH)
51 receptor indirectly represses ciliary localization of Smoothened (SMO), maintaining the
52 pathway in an inactive state. This repression is reinforced by ciliary GPR161, an orphan
53 constitutively active G-coupled protein receptor and negative regulator of the pathway,
54 which maintains high ciliary cyclic AMP (cAMP) levels which in turn increases protein
55 kinase A (PKA) activity. Increased PKA activity lead to proteolytic cleavage of GLI
56 transcription factors into their repressor forms, maintaining expression of target genes
57 low (8). During pathway stimulation, Hh ligand binds PTCH, promoting its export from
58 the cilium, which results in SMO entry and GPR161 exit. In concert, GLI2/3, KIF7, and
59 Suppressor of Fused (SUFU) localization to the ciliary tip increases, and is associated
60 with reduced GLI2/3 cleavage (9,10). Uncleaved GLI2/3 activator forms translocate to
61 the nucleus and induce transcriptional targets including *GLI1* and *PTCH1* (11,12). In this
62 work, we focus on canonical Hh signaling because it has been implicated in the
63 mechanisms underlying ciliopathies across multiple model systems. We compare two
64 steps in the Hh pathway in immortal cell lines: initial ciliary localization of Hh pathway
65 components and downstream Hh target gene expression.

Materials and Methods

Cell culture

Cell lines were obtained from the American Type Cell Collection (ATCC, www.atcc.org) and grown in cell specific medium. ARPE-19 (ATCC, CRL-2302) and hTERT RPE-1 (ATCC, CRL- 4000) cells were cultured in DMEM/F12 with 10% fetal bovine serum (FBS) and 1% penicillin-streptomycin. HEK293T (ATCC, CRL-3216) cells were cultured in DMEM with 10% FBS and 1% penicillin-streptomycin. NIH/3T3 (ATCC, CRL-1658) cells were cultured in DMEM with 10% bovine calf serum and 1% penicillin-streptomycin. SH-SY5Y (ATCC, CRL-2266) cells were cultured in 1:1 Eagle's Minimum Essential Medium:F12 with 10% FBS and 1% penicillin-streptomycin. 0.05% trypsin was used for all cell dissociation.

Time course assay

For each set of experiments, cells were seeded on pairs of coverslips coated with 0.3mg/mL poly-D-lysine and allowed to grow for 2-3 days, until they reached 60-80% confluency. We define batches as cells that were grown, treated, and collected at the same time. After reaching the desired confluency, we serum starved the first pair of coverslips that would be starved for the longest time point (96- or 72-hours). Serum starvation included removing the complete growth medium, rinsing with PBS, and adding serum free medium. This step was repeated for each time point, with all coverslips from the same cell line and batch collected at the end of the time course (0 hour serum starvation). We placed the plates holding the coverslips on ice for 10 minutes, then fixed coverslips using 4% paraformaldehyde for 5 minutes followed by

88 permeabilization using cold methanol for 3 minutes and stored in PBS at 4°C until ready
89 to stain. We only stained one coverslip from the pair, leaving the replicate available as a
90 backup.

91 For HEK293T cells, we incubated the 0.3 mg/mL poly-D-lysine coated coverslips
92 with 0.05% gelatin for 15-20 minutes prior to seeding cells to promote adhesion since
93 this cell line is semi-adherent. Otherwise, we followed the same seeding and fixation
94 method described above.

95 All plots were generated using Plots of Data and Super Plots of Data (13,14)

96 Hedgehog pathway protein localization

97 Cells in the same batch were seeded on pairs of coverslips and allowed to
98 expand until they reached 60-80% confluency, as above. Cells were serum starved for a
99 total of 48 hours. After the initial 24 hours of serum starvation, we replaced the media
100 on half of the coverslips with serum free medium + 1μM Smoothened Agonist (SAG)
101 (Millipore, 566661). We placed the plates holding the coverslips on ice for 10 minutes,
102 then fixed coverslips using 4% paraformaldehyde for 5 minutes followed by
103 permeabilization using cold methanol for 3 minutes and stored in PBS at 4°C until ready
104 to stain. We only stained one coverslip from the pair, leaving the replicate available as a
105 backup.

106 Quantitative immunofluorescence

107 We blocked coverslips in 2% bovine albumin serum (BSA) in phosphate buffered
108 solution (PBS) for 20 minutes at room temperature. Time course assay coverslips were

109 incubated with mouse anti-acetylated α-tubulin (1:2000, Sigma Aldrich, T6793) and
110 rabbit anti-ARL13B (1:800, Proteintech, 17711-1-AP) antibodies diluted in blocking
111 buffer. Hedgehog pathway protein localization coverslips were incubated with either 1)
112 mouse anti-SMO (1:50, Santa Cruz Biotechnology, sc-166685) and rabbit anti-ARL13B
113 (1:800, Proteintech, 17711-1-AP) antibodies or 2) mouse anti-ARL13B (1:200,
114 NeuroMab, 75-287) and rabbit anti-GPR161 (1:200, Proteintech, 13398-1-AP)
115 antibodies diluted in blocking buffer. Coverslips were incubated with primary antibodies
116 for 1 hour at room temperature or at 4°C overnight, then washed in PBS for 5 minutes,
117 three times. Coverslips were incubated with the following secondary antibodies at 1:400
118 dilution for 1 hour at room temperature: Goat anti-Rabbit IgG, Alexa Fluor 488 (Thermo
119 Fisher Scientific #A11008) and Donkey anti-Mouse IgG, Alexa Fluor 568 (Thermo
120 Fisher Scientific, #A10037). After incubation, we washed coverslips in PBS for 5
121 minutes, three times. Coverslips were mounted on slides using a Fluoromount with
122 DAPI (Invitrogen, #00-4959-52), then sealed with nail polish after sitting for at least 1
123 hour.

124 We quantified ciliary protein localization using a validated protocol previously
125 established in the laboratory (15). We imaged coverslips using the same microscopy
126 settings to acquire z-stack images for >20 cells with cilia for each condition and batch
127 using identical microscope settings. We converted z-stack images to sum-projections
128 and randomized these images using the FIJI (16) script, Filename_randomizer
129 (https://imagej.nih.gov/ij/macros/Filename_Randomizer.txt) to minimize bias between
130 cell lines and conditions. Prior to data collection, we checked a subset of images to ensure
131 that the cilium marker (ARL13B) and protein of interest (SMO or GPR161) signals were

132 adequate for measurement. Blinded to the condition, we drew a cilium mask in the cilium marker
133 channel (ARL13B) using summed Z-stack images in ImageJ. We used this mask to measure
134 the signal intensity for the protein of interest and measured the signal intensity of an
135 adjacent region to subtract background signal. Normalized fluorescence intensity was
136 calculated using the following formula:

137 $$\frac{(Un)stimulated\ (Cilium\ average\ fluorescence\ intensity - Background\ average\ fluorescence\ intensity)}{\bar{x}\ Unstimulated\ (Cilium\ average\ fluorescence\ intensity - Background\ average\ fluorescence\ intensity)}$$

138 Finally, we unblinded the data and visually inspected the images to ensure that
139 our qualitative assessment of ciliary signal was consistent with the quantitative data. We
140 also used the same data set to determine proportion of cells with cilia and cilium length
141 in baseline and stimulated cells.

142 *GLI1* and *PTCH1* qPCR

143 Cells were grown in pairs of T-75 cell culture flasks until 60-80% confluent, then
144 starved for a total of 48 hours. After the initial 24 hours, half the flasks had their media
145 replaced with serum free medium + 1μM SAG. We dissociated the cells and extracted
146 RNA using the Aurum Total RNA mini kit (Biorad, 7326820). We measured RNA
147 concentration using a spectrophotometer and only included RNA that had an A260/280
148 >1.8. cDNA was generated using the BioRad iScript cDNA Synthesis kit. We set up
149 qPCR reactions using the PowerUp SYBR Green Master Mix (Thermo Fisher Scientific,
150 #A25741). For cell lines that required the touchdown qPCR protocol, we followed the
151 protocol outlined in Zhang et al. (17). Briefly, the touchdown qPCR protocol went as
152 follows: 50C (2 min), 95C (2 min), 4x [95C (20 sec), 65C (10 sec, decrease 3C/cycle,
153 72C (1 min)], 40x [95C (15 sec), 55C (15 sec), 72C (1 min)], ending with a melt

154 temperature curve. qPCR data acquisition was performed on the Bio-Rad CFX96 Touch
155 Real-Time PCR Detection System.

156 Human *GLI1* primers

157 Forward 5'-GATGACCCCACCACCAATCAGTAG-3'

158 Reverse 5'-AGACAGTCCTTCTGTCCCCACA-3'

159 Human *PTCH1 primers*

160 Forward 5'-GAGCACTTCAAGGGGTACGA-3'

161 Reverse 5'-GGAAAGCACCTTTTGAGTGG-3'

162 Mouse *Gli1* primers

163 Forward 5'-CCGACGGAGGTCTCTTTGTC-3'

164 Reverse 5'-GCGTCTCAGGGAAGGATGAG-3'

165 Human *Ptch1 primers*

166 Forward 5'-GAGCAGATTTCCAAGGGGAAG -3'

167 Reverse 5'-CCACAACCAAAAACTTGCCG -3'

168 Reference gene identification

169 To ensure robust data acquisition, we identified an ideal reference gene for each
170 cell line. We identified 10 human candidate reference genes and 9 mouse candidate
171 reference genes (Table 1) to evaluate expression stability between baseline and
172 stimulated cDNA. To select a reference gene, we evaluated the cycle threshold (CT) of
173 three starting primer concentrations, and cDNA dilution curve efficiency (18).

174 **Table 1. Candidate qPCR reference gene names and primer sequences.**

Gene symbol	Gene name	Forward and Reverse Primer
ACTB	Actin Beta	5'-GAGCACAGAGCCTCGCCTTT-3'

		5'-TCATCATCCATGGTGAGCTGG-3'
GAPDH	Glyceraldehyde 3-phosphate dehydrogenase	5'-AGGTGAAGGTCGGAGTCAAC-3' 5'-TTCACACCCATGACGAACAT-3'
IPO8	Importin 8	5'-TGCAGTCCGGCCTACTGTTC-3' 5'-TGTAGGACTGGTTGAGCTCGTTC-3'
PUM1	Pumillio RNA Binding Family Member	5'-AAGGACAGCAGCAGGTTCTC-3' 5'-CCTTGTCCAAATGCAAGGGC-3'
RPLP0	Ribosomal Protein Lateral Stalk Subunit P0	5'-CGTCCTCGTGGAAGTGACAT-3' 5'-TAGTTGGACTTCCAGGTCGC-3'
SDHA	Succinate dehydrogenase complex flavoprotein subunit A	5'-GCATTTGGCCTTTCTGAGGC-3' 5'-TTGATTCCTCCCTGTGCTGC-3'
TBP	TATA Binding Protein	5'-GTGACCCAGCATCACTGTTTC-3' 5'-AGAGCATCTCCAGCACACTC-3'
UBC	Ubiquitin C	5'-CCGGGATTTGGGTCGCAG-3' 5'-TCACGAAGATCTGCATTGTCAAG-3'
YWHAZ	Tryosine 3-Monooygenase.Tryptophan 5-Monooygenase Activation Protein Zeta	5'-GACACAGAACATCCAGTCATGG-3' 5'-TCATATCGCTCAGCCTGCTC-3'
18S(19)	18S rRNA	5'-AGAAACGGCTACCACATCCA-3' 5'-CACCAGACTTGCCCTCCA-3'
Actb	Actin Beta	5'-TAGGCACCAGGGTGTGATG-3' 5'-TCTCCATGTCGTCCCAGTTG-3'
Gapdh	Glyceraldehyde 3-phosphate dehydrogenase	5'-AATGTGTCCGTCGTGGATCT-3' 5'-ATACGGCTACAGCAACAGGG-3'
Ipo8	Importin 8	5'-ACAAGCTCTGCTGACTGTGC-3' 5'-CAGTGTCCTTCGGTGCTCTG-3'
Pum1	Pumillio RNA Binding Family Member	5'-GAAAGGTAAGGGGGAGCGAG-3' 5'-CTCATTCCACCAACACGGGC-3'
Rplp0	Ribosomal Protein Lateral Stalk Subunit P0	5'-TCCTCGTTGGAGTGACATCG-3' 5'-AGTTGGACTTCCAGGTCGC-3'
Sdha	Succinate dehydrogenase complex flavoprotein subunit A	5'-ACTGTTATTGCTACTGGGGGC-3' 5'-CCCTAGTGACCATGGCTGTG-3'
Tbp	TATA Binding Protein	5'-GGTATCTGCTGGCGGTTTGG-3' 5'-GAAATAGTGATGCTGGGCACTG-3'
Ubc	Ubiquitin C	5'-CCCACACAAAGCCCCTCAAT-3' 5'-AAGATCTGCATCGTCTCTCTCACG-3'
Ywhaz	Tryosine 3-Monooygenase.Tryptophan 5-Monooygenase Activation Protein Zeta	5'-GGTATCTGCTGGCGGTTTGG-3' 5'-GAAATAGTGATGCTGGGCACTG-3'

We included 10 candidate reference genes for human-derived cell lines and 9 candidate gene reference genes for the NIH/3T3 murine-derived cell line.

In our initial screen, we were looking for 1) small ΔCT between unstimulated and stimulated within each cell line, indicating unchanged expression level between experimental conditions, and 2) a CT between 20-30 cycles so that expression levels were similar to *GLI1* and *PTCH* expression. We optimized primer concentration by diluting forward and reverse primers sets to three concentrations, 3μM, 5μM, and 7μM. Next, we determined primer efficiency by performing a cDNA dilution series. We followed widely accepted primer efficiency standards, which includes an efficiency of 80-120% and $R^2 \geq 0.99$.

During assay validation, we determined that *GLI1* in ARPE-19, HEK293T, and NIH/3T3 cells amplified at >29 cycles, close to the limit of reliable detection; therefore, we performed a modified qPCR assay in these cell lines, which included a touchdown step prior to the 40-cycle amplification. This lowered the detection level by 3 cycles in ARPE-19 and HEK293T cells. In NIH/3T3 cells, we did not see a difference in unstimulated cycle values and only saw a difference of 1 cycle in stimulated cells.

Statistical analysis

An unpaired two-tailed Student's *t*-test was performed for comparison between unstimulated and stimulated cells with a hypothesized mean difference of 0. α level was set at 0.05. $P < 0.05$ was significant. Symbols for significance represent *p*-values from 0.01 to 0.05 (*), 0.001 to 0.01 (**), and <0.001 (***).

Results

Cell line selection

199 We identified candidate models for human Hh signaling by evaluating the
200 following characteristics in commercially available cell lines: human-derived, evidence of
201 ciliation, immortal, required imaging characteristics (adherent, monolayer growth),
202 evidence of Hh pathway response, and genetic tractability. ARPE-19, HEK293T, hTERT
203 RPE-1, NIH/3T3, and SH-SY5Y cells met most criteria (Table 2). We included murine
204 NIH/3T3 cells as a non-human control since these cells are frequently used to model Hh
205 pathway function (6,20–22).

206 **Table 2. Desired cell line characteristics for modeling Hh signaling.**

	ARPE-19	HEK293T	hTERT RPE-1	SH-SY5Y	NIH/3T3
Cell origin	Retinal pigment epithelial cells	Embryonic kidney cells	Retinal pigment epithelial cells	Bone marrow derived Neuroblast oma cells	Murine embryonic fibroblast cells
Human-derived	Y	Y	Y	Y	N
Ciliated	Y	Y	Y	Y	Y
Immortal	Y	Y	Y	Y	Y
Adherent	Y	S	Y	Y	Y
Monolayer growth	Y	N	Y	N	Y
Hh pathway response	Y	Y	Y	Y	Y

Gross chromosomal abnormalities	N	Y	N	N	N
Genetic tractability	Y	Y	Y	NR	Y

We searched the literature for evidence of the desired characteristics listed. ATCC often provided information about the following categories: human-derived, immortal, gross chromosomal abnormalities. When considering any known response to Hedgehog signaling, this included assays that measured response differently from the assays discussed in this paper (i.e. GLI3 processing, GLI luciferase assays). Y= Yes, N= No, S = semi-adherent, NR= Not reported.

Proportion of cells with cilia

While all the cell lines have been reported to ciliate, the time course of ciliation for different cell lines is scattered across studies (23,24). Therefore, we aimed to define the optimal serum starvation conditions for Hh signaling experiments by determining the proportion of ciliated cells across time points after serum starvation: 0, 8, 16, 24, 48, 72, and 96 hours. Serum starvation removes growth factors available to cells, causing cells to drop out of the cell cycle and promoting ciliogenesis. For Hh imaging assays, we wanted cells to be in a monolayer layer, but we were unable to measure the 96-hour time point for HEK293T cells, because they became overgrown when grown for >72 hours under standard conditions.

Baseline ciliation varied between cell types, ranging from ~5% in SH-SY5Y to ~62% in hTERT RPE-1 (Fig 1). Serum starvation was associated with >15% higher ciliation rates over baseline in ARPE-19, hTERT RPE-1, and NIH/3T3 cell lines. Peak ciliation in these cell lines typically occurred 48 hours post-starvation and ranged from

228 56% in ARPE-19 to 97% in NIH/3T3. In contrast, HEK293T and SH-SY5Y ciliation rates
229 were the same with and without serum starvation.

230 **Fig 1. Ciliation time course and cilia length for immortal cell lines.** A) Proportion of
231 ciliated cells at 0, 8, 16, 24, 48, 72, and 96 hours post serum starvation. The numbers of
232 cells counted at each time point are listed below each column of the graphs. B) Cilium
233 length across time points. Black bars across graphs delineate 2 and 4μm. Black bars in
234 each column represent median length. C) Proportion of ciliated cells without and with
235 stimulation. Each symbol represents the proportion of ciliated cells in one batch. D)
236 Cilium length without stimulation and with stimulation. Large symbols = median cilium
237 length within a batch. Small symbols = cilium length of one cilium. One coverslip was
238 imaged for each cell line and time point. The total number of cells counted across three
239 batches are listed below each column of the graphs.

240 SH-SY5Y cells ciliated at low proportions through 96 hours of starvation,
241 prompting us to evaluate 120- and 144-hour time points to determine whether ciliation
242 was delayed compared to other cell lines. Even with prolonged starvation, <8% of SH-
243 SY5Y cells had cilia at each time point (S1 Fig).

244 We and others have previously documented proportions of ciliated HEK239T
245 cells >20% (25). To determine whether the low proportions of cells with cilia was a
246 characteristic of the specific isolate of HEK293T cells, we repeated the time course
247 experiment using three different isolates of HEK293T cells in our collection (S2A Fig).
248 Baseline ciliation rates were similar to our initial experiment (~20%) and increased to
249 32-39% by 24 hours. At 48 and 72 hours, the proportion of cells with cilia was lower
250 than at 24 hours. We compared images of areas monolayer and multilayer growth,

251 finding that more densely grown areas had more cilia (S2B, S2C Fig). For the Hh
252 experiments described below, we continued with monolayer cultures to allow for
253 accurate quantitative immunofluorescence measurements.

254 Cilium length

255 We measured cilium length across all timepoints (Fig 1B). Cilium length was
256 shorter at 0 hours for ARPE-19, HEK293T, hTERT RPE-1, and NIH/3T3 cells,
257 stabilizing between 8-24 hours, while cilium length was similar across timepoints in SH-
258 SY5Y cells. Maximum median length for each cell line was 3.0μm for ARPE-19, 2.1μm
259 for HEK293T, 3.2μm for hTERT RPE-1, 2.8μm for NIH/3T3, and 1.4μm for SH-SY5Y
260 cells. Based on the low ciliation rate and exceptionally short cilia, we did not continue
261 evaluating SH-SY5Y cells for Hh pathway response.

262 Hedgehog pathway response

263 We next measured canonical Hh pathway activity in the cell lines using two Hh
264 pathway assays commonly reported in the literature: 1) upstream localization of Hh
265 pathway effectors SMO and GPR161 into and out of the cilium, respectively (8,26), and
266 2) downstream target gene (*GLI1* and *PTCH1)* induction (11).

267 Hh pathway protein localization

268 We measured the ciliary localization of SMO and GPR161 in unstimulated and
269 Smoothened agonist (SAG) stimulated cells using our established quantitative
270 immunofluorescence (qIF) protocol that determines relative protein localization between
271 different cell lines and conditions (15).

272 Proportion of cells with cilia and cilium length in response to Hh

stimulation

Proportion of ciliated cells and cilium length were moderately affected by pathway stimulation (Fig 1C, 1D). Proportion of ciliated cell was lower in stimulated cells compared to unstimulated cells across cell lines in a majority of batches. Cilium length was significantly decreased in ARPE-19 and NIH/3T3 cells, significantly increased in hTERT RPE-1 cells, and was not significantly different in HEK293T cells.

SMO localization

Normalized mean ciliary SMO signal was significantly higher in stimulated cells compared to unstimulated cells across all cell lines, with fluorescence intensity reported in arbitrary units (au): 1.5 – 2.6 au in ARPE-19, 1.2 – 2.7 au in HEK293T, 2.1 – 2.9 au in hTERT RPE-1, and 7.0 – 10.3 au in NIH/3T3 cells (Fig 2A). In ARPE-19 and HEK293T cells, SMO ciliary fluorescence intensity was weaker and background signal was higher compared to hTERT RPE-1 and NIH/3T3 cells (S2A Fig).

Fig 2. SMO and GPR161 localization in response to Hh pathway stimulation. Normalized fluorescence intensity (au) of A) SMO and B) GPR161 with and without pathway stimulation. Large symbol = median normalized fluorescence intensity for individual coverslip data. Small symbol = normalized fluorescence intensity of one cilium. Measurement from three separate batches are indicated by a unique symbol shape and color. Total number of cilia measured listed in the second row below the graph. Representative images are shown below graphs for unstimulated (-SAG) and stimulated (+SAG) cells. Two-tailed Student's *t*-test was performed. *P*-values represented significant differences if they ranged from 0.01 to 0.05 (*), 0.001 to 0.01 (**), and <0.001 (***).

296 ## GPR161 localization

297 We detected cilium-specific GPR161 signal in HEK293T and hTERT RPE-1 cells,
298 a faint cilium-specific signal in ARPE-19 cells, and no cilium-specific signal in NIH/3T3
299 cells (Fig 2B), so we could not measure GPR161 response in NIH/3T3 cells. Across
300 three batches, normalized mean GPR161 intensity was lower with SAG stimulation:
301 0.57- 0.73 au in ARPE-19, 0.64 - 0.76 au in HEK293T, and 0.40 – 0.95 au in hTERT
302 RPE-1 (Fig 2B). For one of the three hTERT RPE-1 passages (Batch 3), the GPR161
303 signal was the same with and without stimulation. We suspect that this was due to an
304 undetermined technical issue since hTERT RPE-1 cells responded when we repeated
305 the experiment on an additional passage (S2C Fig).

306 ## Hh target gene expression

307 *GLI1* and *PTCH1* are direct transcriptional outputs of the canonical Hh pathway
308 and are commonly used to measure pathway activity (11). To measure *GLI1* and
309 *PTCH1* expression, we optimized our quantitative PCR assays using the $2^{-\Delta\Delta CT}$ method
310 (27).

311 To accurately measure transcriptional responses to pathway stimulation using
312 the $2^{-\Delta\Delta CT}$ quantitative PCR method, we identified suitable reference genes whose
313 expression levels were similar to *GLI1* and *PTCH1* (>20 cycles, <30 cycles) and did not
314 change with pathway stimulation in each cell line. We searched the literature for
315 commonly used reference genes, identifying ten candidates for human cell lines and
316 nine candidates for the mouse cell line (primers listed in Methods). We chose the genes
317 with the most similar expression levels in stimulated and unstimulated cells, with the
318 amplification cycles closest to *GLI1* and *PTCH1*: *PUM1* for ARPE-19 cells, *TBP* and

319 *PMBS* for HEK293T cells, *TBP* for hTERT RPE-1 cells, and *Sdha* for NIH/3T3 cells (S4
320 Fig). We also used murine specific *Gli1* and *Ptch1* primer sets for NIH/3T3 cells.
321 Although we tested *TBP* and *PMBS* for HEK293T, and used *PMBS* in our experiment,
322 neither was ideal: *TBP* expression was variable in stimulated cells, and *PMBS*
323 expression varied with stimulation in one out of the three batches (S4 Fig).

324 In hTERT RPE-1 cells, *GLI1* expression was 2.8 to 3.8-fold higher and *PTCH1*
325 expression was 1.7 to 1.9-fold higher with stimulation (Fig 3). In contrast, stimulation
326 was not associated with marked expression differences in ARPE-19 cells (*GLI1* 0.9 to
327 1.4-fold, *PTCH1* 1.0 to 1.1-fold) or HEK293T cells (*GLI1* 0.5 to 1.7-fold, *PTCH1* 0.3 to
328 0.7 fold), consistent with the lack of relocalization of SMO and GPR161 with SAG
329 stimulation. Strikingly, *Gli1* expression was 1993 to 3034-fold higher with stimulation in
330 NIH/3T3 cells. Similarly, *Ptch1* expression was also markedly higher (46 to 70-fold).

331 **Fig 3. *GLI1* and *PTCH1* expression in response to Hh pathway stimulation.** A) *GLI1*
332 and B) *PTCH1* target gene induction. Each data point represents the expression fold
333 change of stimulated cells from the same batch. Expression fold change was
334 normalized to unstimulated values, which were set to 1. Two-tailed Student's *t*-test was
335 performed. *P*-values represented significant differences if they ranged from 0.01 to 0.05
336 (*), 0.001 to 0.01 (**), and <0.001 (***).

337 Discussion

338 This systematic evaluation of cilium characteristics and Hh signaling in five
339 commercially available, immortal, mammalian cell lines revealed that hTERT RPE-1 and
340 NIH/3T3 cells are suitable for modeling Hh signaling (Table 3). By using the same
341 assays in different cell types, we determined differences in response to Hh stimulation.

342 Based on our experiments, SH-SY5Y cells were not suitable because of their low
343 ciliation rate and very short cilia. ARPE-19 and HEK239T cells localizaed the Hh
344 pathway proteins SMO and GPR161 in response to stimulation; however, they did not
345 upregulate the Hh target genes *GLI1* and *PTCH1.* Only hTERT RPE-1 and NIH/3T3
346 cells ciliated well and showed robust responses to stimulation in both sets of assays.
347 Our experiments also demonstrate that Hh pathway stimulation moderately impacts
348 ciliation rates and cilium length across all of the cell lines, but not in a consistent manner
349 across batches. We observed a range of responses to stimulation, from minimally
350 responsive (ARPE-19 and HEK293T), to modestly responsive (hTERT RPE-1) to
351 robustly responsive (NIH/3T3) (Table 3). It is not clear whether this represents species-
352 specific or cell line-specific differences, but it does indicate that results should be
353 validated across model systems before they can be considered generalizable.

354 **Table 3. Overview of results.**

	Max proportion of cells with cilia	**Cilium length (mean)**	**SMO and GPR161 response to stimulation**	***GLI1*/*PTCH1* induction**
ARPE-19	65% (72 hr)	3.0μm	SMO: ↑2.50-fold GPR161: ↓0.25-fold	*GLI1*: ND *PTCH1*: ND
HEK293T	22% (24 hr)[1]	2.0μm	SMO: ↑2.50-fold GPR161: ↓0.25-fold	*GLI1*: ND *PTCH1*: ND
hTERT RPE-1	80% (72 hr)	3.1μm	SMO: ↑2.50-fold GPR161: ↓0.50-fold	*GLI1*: ↑3-fold *PTCH1*: ↑2-fold
NIH/3T3	97% (48 hr)	2.9μm	SMO: ↑9.50-fold GPR161: ND	*GLI1*: ↑3000-fold *PTCH1*: ↑60-fold
SH-SY5Y	8% (16 hr)	1.3μm		

355 We summarized the outcome of our ciliary characterization and Hedgehog assays.
356 hTERT RPE-1 cells were the most response human-derived cell line and NIH/3T3 cells
357 were the most responsive cell line overall. We did not measure SH-SY5Y response to
358 Hedgehog signaling because of low proportion of ciliated cells and short cilia.

359 [1]In follow-up experiments, proportion of ciliated cells was increased by allowing cells to
360 grow at a higher density.

361 It is also clear from our experiments that each Hh assay requires optimization for
362 each cell line. Prior to assessing Hh response, we had to determine acceptable
363 seeding, growth conditions, and fixation. In HEK293T cells, we had to balance the
364 upside of higher ciliation rates in confluent cultures with the downside of overlapping
365 cells complicating qIF measurements; therefore, low ciliation rates in HEK293T cells
366 may have contributed to the low Hh target gene induction.

367 For our qIF experiments, we had to identify antibodies that worked across cell
368 lines and were specific to the protein of interest. The limited response to SAG
369 stimulation in ARPE-19 and HEK293T cells could be due to difference in expression of
370 Hh negative regulators in these cell lines that differ from hTERT RPE-1 and NIH/3T3
371 cells, for example SUFU expression which complexes with GLI2/3 and stabilizes the
372 activator forms of the proteins (28). Alternatively, these cells might respond to native Hh
373 ligand or other agonists, but not SAG. There is prior evidence that hTERT RPE-1 and
374 NIH/3T3 cells relocalize SMO and GPR161 and upregulate pathway target genes in
375 response to Hh stimulation (22,29,30). ARPE-19 cells have been used to determine Hh
376 response to cyclopamine, a down-regulator of the pathway (31). We could not detect
377 Gpr161 in NIH/3T3 cells by immunofluorescence, despite the 94% amino acid identity
378 between the human and mouse for the antigen used to generate the antibody. This may
379 be due to differences between the human and mouse proteins at the key epitopes
380 recognized by the polyclonal antibody. Alternatively, Gpr161 expression has been
381 demonstrated in other studies using different stimulation time points (32). Future work
382 could explore ligand dose-response, and optimal timing for SMO and GPR161
383 localization in response to Hh stimulation.

384 qPCR also needs to be tailored to each line. We optimized primer sets, template
385 concentrations, and amplification parameters. Importantly, expression of the commonly
386 used reference gene, *GAPDH,* differed between unstimulated and stimulated HEK293T
387 cells. *GAPDH* expression responds to serum starvation (33,34), adding to the
388 importance of screening reference genes for each cell line. During *GLI1* primer
389 optimization, we identified high CT values in our cell lines (>30 CT), which introduces
390 variability (35). To bring the CT values into a better range, we increased template
391 concentration and added a touchdown step in ARPE-19 and HEK293T, lowering the CT
392 values by 3-4 cycles(17). Unstimulated NIH/3T3 samples also had a CT >30, but the
393 touchdown step did not decrease CT values in this cell line, suggesting the *GLI1*
394 expression is below the level of detection in this cell line and increases substantially
395 with stimulation.
396 While we confirmed that hTERT RPE-1 and NIH/3T3 cells are appropriate cell
397 lines to model Hh signaling, we have not demonstrated that they recapitulate all aspects
398 of Hh signaling across cell types *in vivo*; therefore, Hh experiments in these cell lines
399 should be validated in additional models, ideally *in vivo*. In addition, we have not fully
400 excluded ARPE-19 and HEK293T cells as potential models, since we did not evaluate
401 all aspects of Hh signaling such as dose-response to ligand, time course, and other
402 important characteristics. If there were compelling reasons to use these cell lines for
403 Hh-related experiments, further characterization might reveal intact Hh responses at
404 different timepoints or different agonist concentrations.
405 hTERT RPE-1 and NIH/3T3 cells respond consistently to Hh pathway stimulation
406 across two standard assays and are genetically tractable. These cell lines provide

407 models originating from two organisms and could be used individually or in parallel to
408 study Hh response. hTERT RPE-1 cells are a good model system for exploring these
409 mechanistic details at the cellular level.

410 References

411 1. Berbari NF, O'Connor AK, Haycraft CJ, Yoder BK. The primary cilium as a complex
412 signaling center. Curr Biol CB. 2009 Jul 14;19(13):R526-535.

413 2. Goetz SC, Anderson KV. The primary cilium: a signalling centre during vertebrate
414 development. Nat Rev Genet. 2010 May;11(5):331–44.

415 3. Pietrobono S, Franci L, Imperatore F, Zanini C, Stecca B, Chiariello M. MAPK15
416 Controls Hedgehog Signaling in Medulloblastoma Cells by Regulating Primary
417 Ciliogenesis. Cancers. 2021 Sep 29;13(19):4903.

418 4. Yoon JW, Gallant M, Lamm MLG, Iannaccone S, Vieux K-F, Proytcheva M, et al.
419 Noncanonical regulation of the Hedgehog mediator GLI1 by c-MYC in Burkitt
420 lymphoma. Mol Cancer Res MCR. 2013 Jun;11(6):604–15.

421 5. Hulleman JD, Nguyen A, Ramprasad VL, Murugan S, Gupta R, Mahindrakar A, et
422 al. A novel H395R mutation in MKKS/BBS6 causes retinitis pigmentosa and
423 polydactyly without other findings of Bardet-Biedl or McKusick-Kaufman syndrome.
424 Mol Vis. 2016;22:73–81.

425 6. Breslow DK, Hoogendoorn S, Kopp AR, Morgens DW, Vu BK, Kennedy MC, et al.
426 A CRISPR-based screen for Hedgehog signaling provides insights into ciliary
427 function and ciliopathies. Nat Genet. 2018 Mar;50(3):460–71.

428 7. Briscoe J, Thérond PP. The mechanisms of Hedgehog signalling and its roles in
429 development and disease. Nat Rev Mol Cell Biol. 2013 Jul;14(7):416–29.

430 8. Mukhopadhyay S, Wen X, Ratti N, Loktev A, Rangell L, Scales SJ, et al. The
431 Ciliary G-Protein-Coupled Receptor Gpr161 Negatively Regulates the Sonic
432 Hedgehog Pathway via cAMP Signaling. Cell. 2013 Jan 17;152(1):210–23.

433 9. He M, Subramanian R, Bangs F, Omelchenko T, Liem KF, Kapoor TM, et al. The
434 kinesin-4 protein Kif7 regulates mammalian Hedgehog signalling by organizing the
435 cilium tip compartment. Nat Cell Biol. 2014 Jul;16(7):663–72.

436 10. Wen X, Lai CK, Evangelista M, Hongo J-A, de Sauvage FJ, Scales SJ. Kinetics of
437 Hedgehog-Dependent Full-Length Gli3 Accumulation in Primary Cilia and
438 Subsequent Degradation. Mol Cell Biol. 2010 Apr 15;30(8):1910–22.

439 11. Platt KA, Michaud J, Joyner AL. Expression of the mouse Gli and Ptc genes is
440 adjacent to embryonic sources of hedgehog signals suggesting a conservation of
441 pathways between flies and mice. Mech Dev. 1997 Mar;62(2):121–35.

442 12. Haycraft CJ, Banizs B, Aydin-Son Y, Zhang Q, Michaud EJ, Yoder BK. Gli2 and
443 Gli3 localize to cilia and require the intraflagellar transport protein polaris for
444 processing and function. PLoS Genet. 2005 Oct;1(4):e53.

445 13. Postma M, Goedhart J. PlotsOfData—A web app for visualizing data together with
446 their summaries. PLOS Biol. 2019 Mar 27;17(3):e3000202.

447 14. Goedhart J. SuperPlotsOfData—a web app for the transparent display and
448 quantitative comparison of continuous data from different conditions. Pollard T,
449 editor. Mol Biol Cell. 2021 Mar 15;32(6):470–4.

450 15. Slaats GG, Isabella CR, Kroes HY, Dempsey JC, Gremmels H, Monroe GR, et al.
451 MKS1 regulates ciliary INPP5E levels in Joubert syndrome. J Med Genet. 2016
452 Jan;53(1):62–72.

453 16. Schindelin J, Arganda-Carreras I, Frise E, Kaynig V, Longair M, Pietzsch T, et al.
454 Fiji: an open-source platform for biological-image analysis. Nat Methods. 2012 Jun
455 28;9(7):676–82.

456 17. Zhang Q, Wang J, Deng F, Yan Z, Xia Y, Wang Z, et al. TqPCR: A Touchdown
457 qPCR Assay with Significantly Improved Detection Sensitivity and Amplification
458 Efficiency of SYBR Green qPCR. PLOS ONE. 2015 Jul 14;10(7):e0132666.

459 18. Bustin SA, Benes V, Garson JA, Hellemans J, Huggett J, Kubista M, et al. The
460 MIQE guidelines: minimum information for publication of quantitative real-time PCR
461 experiments. Clin Chem. 2009 Apr;55(4):611–22.

462 19. Jacob F, Guertler R, Naim S, Nixdorf S, Fedier A, Hacker NF, et al. Careful
463 selection of reference genes is required for reliable performance of RT-qPCR in
464 human normal and cancer cell lines. PloS One. 2013;8(3):e59180.

465 20. Guo S, Liao H, Liu J, Liu J, Tang F, He Z, et al. Resveratrol Activated Sonic
466 Hedgehog Signaling to Enhance Viability of NIH3T3 Cells in Vitro via Regulation of
467 Sirt1. Cell Physiol Biochem Int J Exp Cell Physiol Biochem Pharmacol.
468 2018;50(4):1346–60.

469 21. Kilander MBC, Wang C-H, Chang C-H, Nestor JE, Herold K, Tsai J-W, et al. A rare
470 human CEP290 variant disrupts the molecular integrity of the primary cilium and
471 impairs Sonic Hedgehog machinery. Sci Rep. 2018 Nov 26;8(1):17335.

472 22. Rohatgi R, Milenkovic L, Scott MP. Patched1 Regulates Hedgehog Signaling at the
473 Primary Cilium. Science. 2007 Jul 20;317(5836):372–6.

474 23. Westlake CJ, Baye LM, Nachury MV, Wright KJ, Ervin KE, Phu L, et al. Primary
475 cilia membrane assembly is initiated by Rab11 and transport protein particle II
476 (TRAPPII) complex-dependent trafficking of Rabin8 to the centrosome. Proc Natl
477 Acad Sci U S A. 2011 Feb 15;108(7):2759–64.

478 24. Kim S, Zaghloul NA, Bubenshchikova E, Oh EC, Rankin S, Katsanis N, et al. Nde1-
479 mediated inhibition of ciliogenesis affects cell cycle re-entry. Nat Cell Biol. 2011
480 Apr;13(4):351–60.

481 25. Takahashi K, Nagai T, Chiba S, Nakayama K, Mizuno K. Glucose deprivation
482 induces primary cilium formation through mTORC1 inactivation. J Cell Sci
483 [Internet]. 2018 Jan 8 [cited 2021 Jun 22];131(1). Available from:
484 https://doi.org/10.1242/jcs.208769

485 26. Corbit KC, Aanstad P, Singla V, Norman AR, Stainier DYR, Reiter JF. Vertebrate
486 Smoothened functions at the primary cilium. Nature. 2005 Oct 13;437(7061):1018–
487 21.

488 27. Livak KJ, Schmittgen TD. Analysis of relative gene expression data using real-time
489 quantitative PCR and the 2(-Delta Delta C(T)) Method. Methods San Diego Calif.
490 2001 Dec;25(4):402–8.

491 28. Wang C, Pan Y, Wang B. Suppressor of fused and Spop regulate the stability,
492 processing and function of Gli2 and Gli3 full-length activators but not their
493 repressors. Dev Camb Engl. 2010 Jun;137(12):2001–9.

494 29. Frasca A, Spiombi E, Palmieri M, Albizzati E, Valente MM, Bergo A, et al. MECP2
495 mutations affect ciliogenesis: a novel perspective for Rett syndrome and related
496 disorders. EMBO Mol Med. 2020 Jun 8;12(6):e10270.

497 30. Hey CAB, Larsen LJ, Tümer Z, Brøndum-Nielsen K, Grønskov K, Hjortshøj TD, et
498 al. BBS Proteins Affect Ciliogenesis and Are Essential for Hedgehog Signaling, but
499 Not for Formation of iPSC-Derived RPE-65 Expressing RPE-Like Cells. Int J Mol
500 Sci. 2021 Jan 29;22(3):1345.

501 31. Duan F, Lin M, Li C, Ding X, Qian G, Zhang H, et al. Effects of inhibition of
502 hedgehog signaling on cell growth and migration of uveal melanoma cells. Cancer
503 Biol Ther. 2014 May;15(5):544–59.

504 32. Hong S-R, Wang C-L, Huang Y-S, Chang Y-C, Chang Y-C, Pusapati GV, et al.
505 Spatiotemporal manipulation of ciliary glutamylation reveals its roles in intraciliary
506 trafficking and Hedgehog signaling. Nat Commun. 2018 Apr 30;9(1):1732.

507 33. Schmittgen TD, Zakrajsek BA. Effect of experimental treatment on housekeeping
508 gene expression: validation by real-time, quantitative RT-PCR. J Biochem Biophys
509 Methods. 2000 Nov 20;46(1–2):69–81.

34. Krzystek-Korpacka M, Hotowy K, Czapinska E, Podkowik M, Bania J, Gamian A, et al. Serum availability affects expression of common house-keeping genes in colon adenocarcinoma cell lines: implications for quantitative real-time PCR studies. Cytotechnology. 2016 Dec;68(6):2503–17.

35. Taylor SC, Nadeau K, Abbasi M, Lachance C, Nguyen M, Fenrich J. The Ultimate qPCR Experiment: Producing Publication Quality, Reproducible Data the First Time. Trends Biotechnol. 2019 Jul;37(7):761–74.

Supporting information

S1 Fig. Extended SH-SY5Y ciliation time course. Proportion of ciliated cells for SH-SY5Y cells from 0-144 hours. One coverslip was imaged for each timepoint, with number of cells counted at each time point listed below each column in the graph.

S2 Fig. HEK293T ciliation data. A) Proportion of ciliated HEK293T cells at 0, 24, 48, and 72 hours post serum starvation from additional thaws. B) Representative images of monolayer areas of HEK293T cell growth from Figure 1 (top row) and repeat experiments with additional thaws of HEK293T cells. Cilia were stained with anti-ARL13B antibody. C) Representative images displaying ciliation in areas with multi-layer growth from additional thaws of HEK293T cells. Cilia were stained with anti-ARL13B antibody. Scale bars are 10μm.

S3 Fig. GPR161 and SMO localization. Representative images from each batch showing variation in A) SMO and B) GPR161 localization. C) Normalized fluorescence intensity (arbitrary units, au) of GPR161 with and without stimulation in an additional passage of hTERT RPE-1 cells. Black bars = median normalized fluorescence intensity. Small symbol = normalized fluorescence intensity of one cilium. Numbers of cilia measured are listed below each column in the graph. Representative cilia are shown next to the graphs for unstimulated (-SAG) and stimulated (+SAG) cells. Scale bars are

536 5 μm. T-test of equal variances was performed. p-values: * 0.01 to 0.05, ** 0.001 to
537 0.01, and *** <0.001.

538 **S4 Fig. Variable *GLI1, PTCH1,* and reference gene expression in response to Hh**
539 **pathway stimulation.** *GLI1, PTCH1,* and reference gene CT (cycle threshold) for
540 ARPE-19, HEK293T, hTERT RPE-1, and NIH/3T3 cell lines with and without
541 stimulation. For cell lines with high CT values (>29), we used a touchdown qPCR
542 method. For each condition (with or without stimulation), we collected mRNA from three
543 batches for each cell line. Normalized *GLI1* and *PTCH1* expression for each qPCR
544 condition is on the far right. Each symbol in the left panels represents the average CT
545 from three technical replicates for each batch. Each symbol in the right panels
546 represents the expression fold change for each batch.

547 **S1 Data. Experimental data sets.**

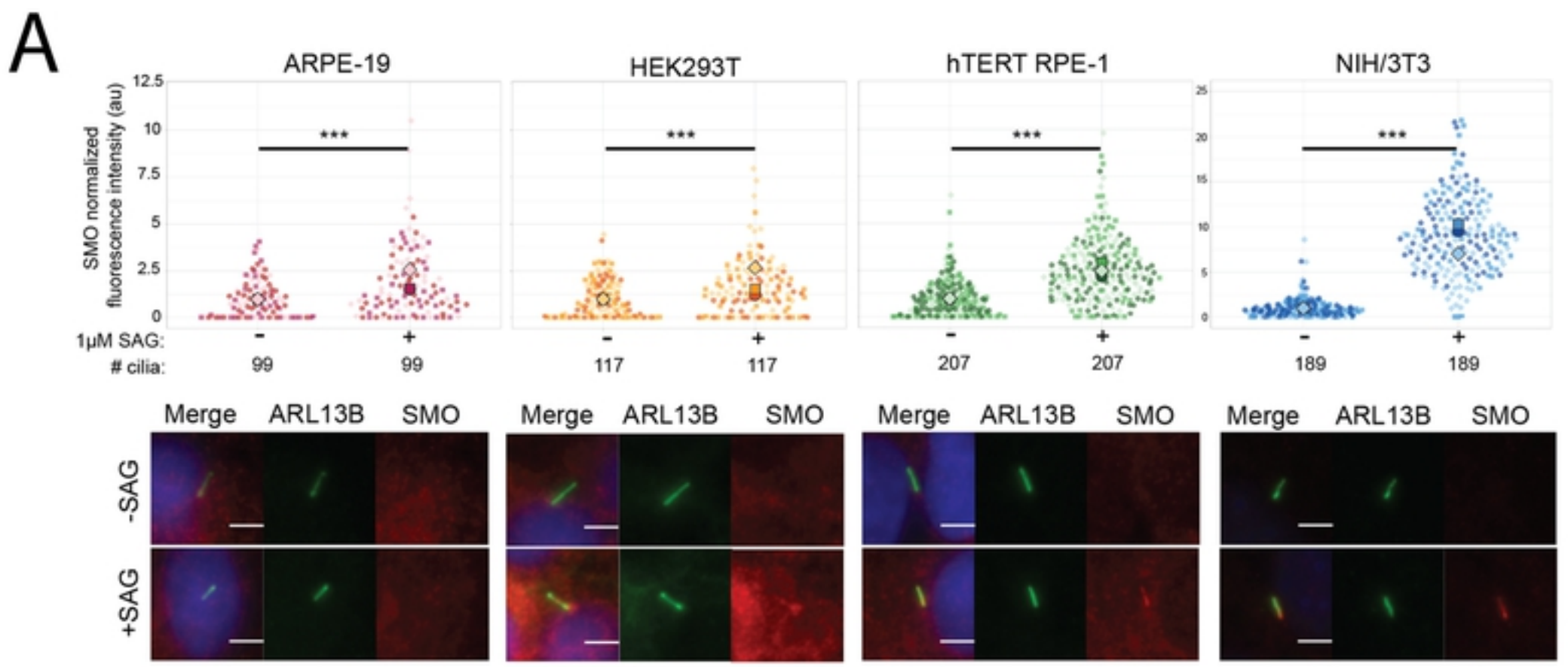
A
ARPE-19
HEK293T
hTERT RPE-1
NIH/3T3
SMO normalized fluorescence intensity (au)
***
1μM SAG:
cilia:
99
99
117
117
207
207
189
189
Merge
ARL13B
SMO
-SAG
+SAG

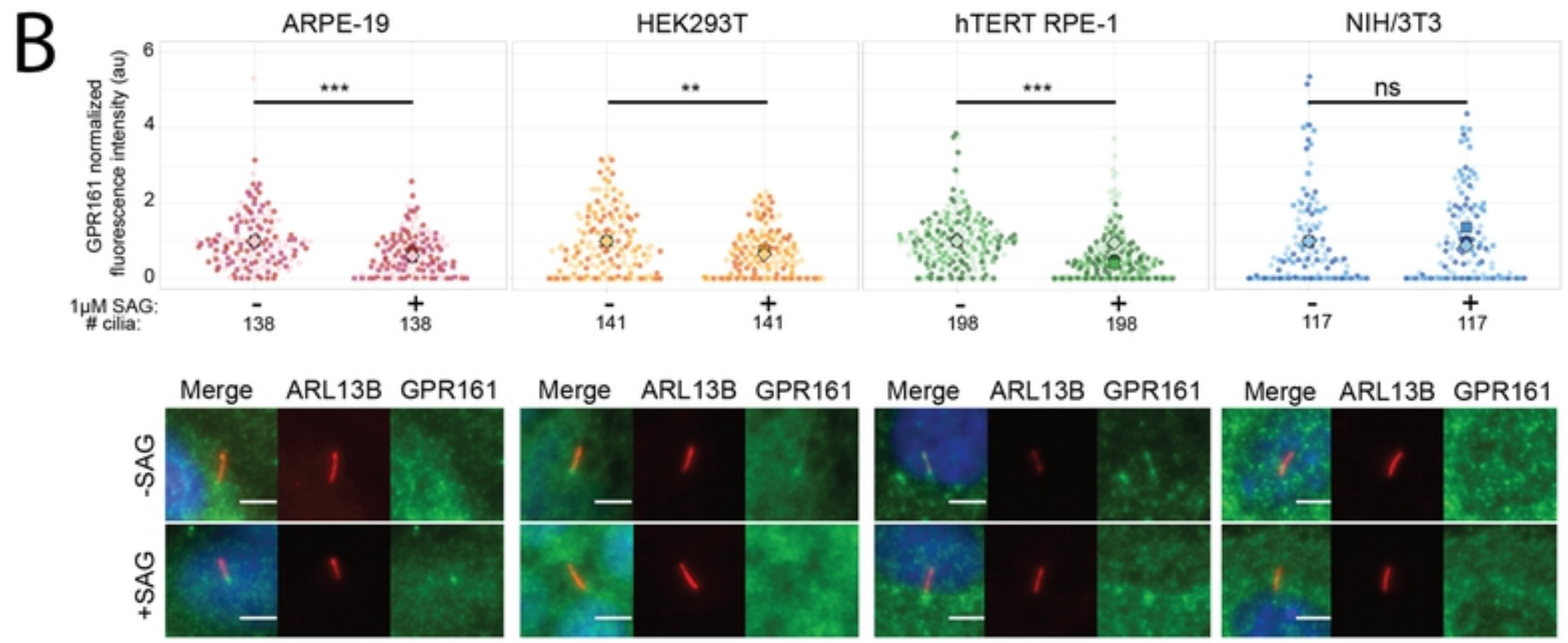
B
ARPE-19
HEK293T
hTERT RPE-1
NIH/3T3
GPR161 normalized fluorescence intensity (au)
***
**
ns
1μM SAG:
cilia:
138
138
141
141
198
198
117
117
Merge
ARL13B
GPR161
-SAG
+SAG

Figure 2

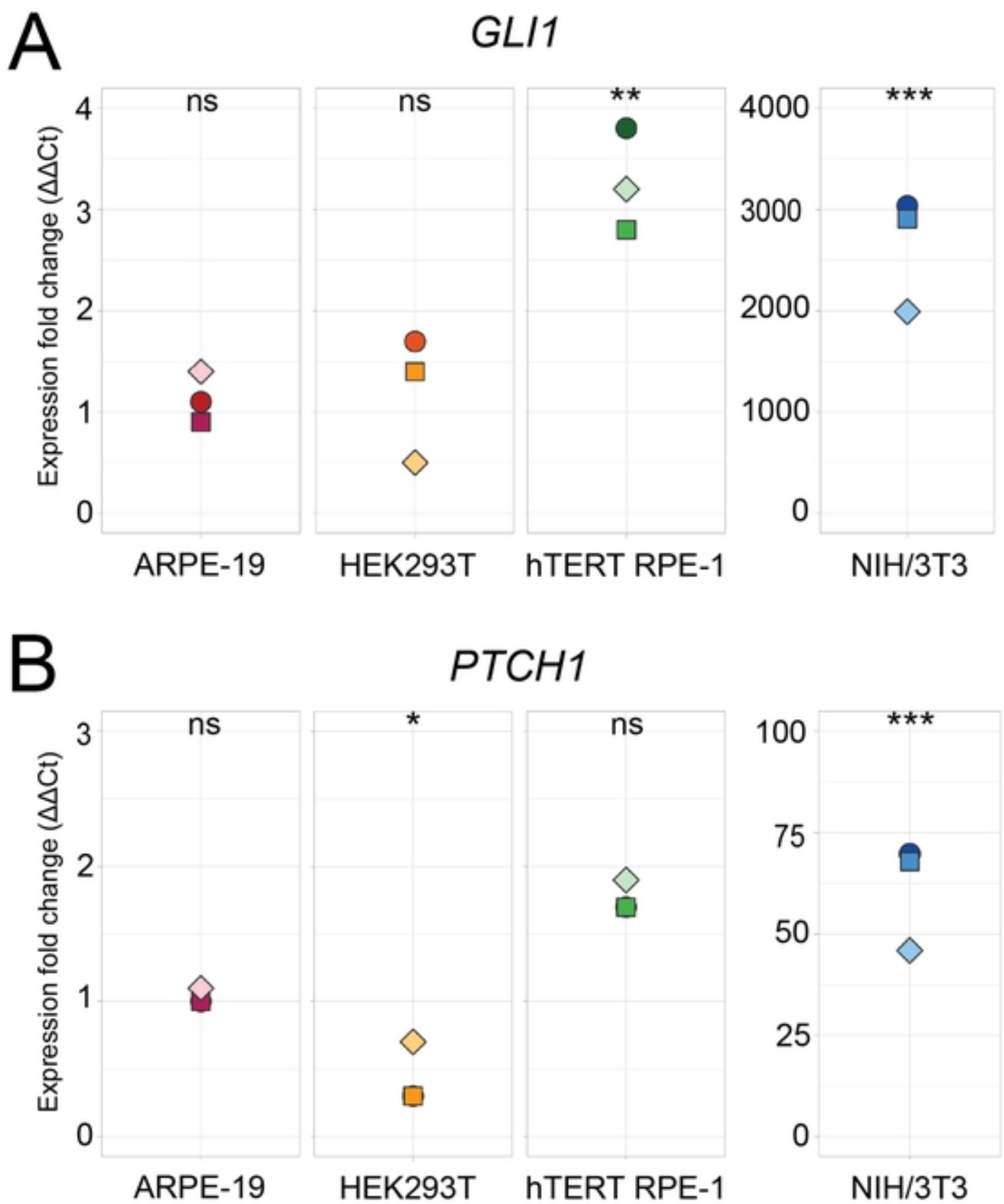
A
GLI1
Expression fold change (ΔΔCt)
ns
ns
**
***
ARPE-19
HEK293T
hTERT RPE-1
NIH/3T3
B
PTCH1
Expression fold change (ΔΔCt)
ns
*
ns
***
ARPE-19
HEK293T
hTERT RPE-1
NIH/3T3

Figure 3

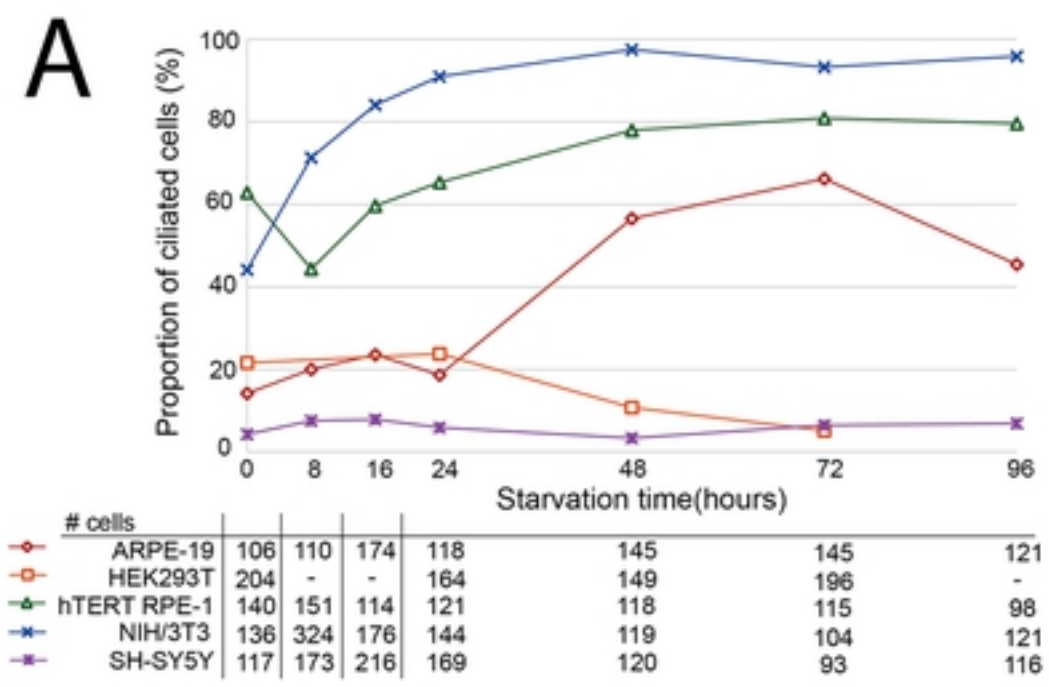
A
Proportion of ciliated cells (%)
Starvation time(hours)
cells
ARPE-19 106 110 174 118 145 145 121
HEK293T 204 - - 164 149 196 -
hTERT RPE-1 140 151 114 121 118 115 98
NIH/3T3 136 324 176 144 119 104 121
SH-SY5Y 117 173 216 169 120 93 116

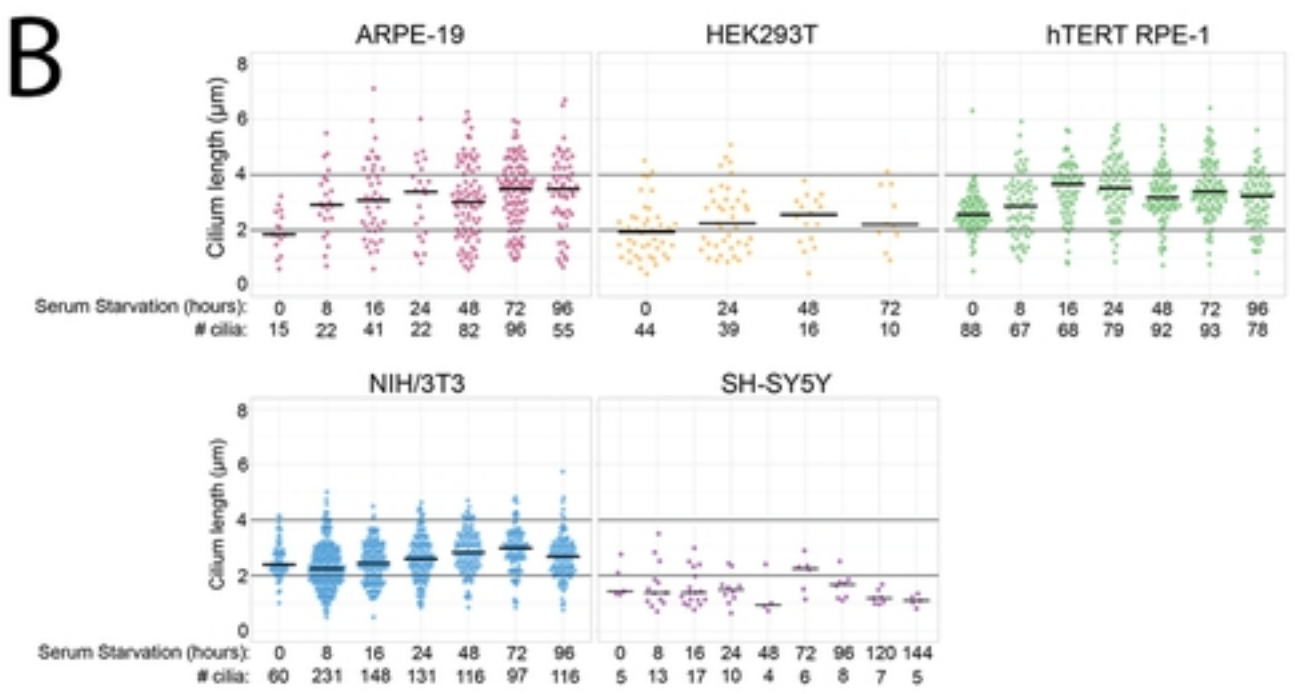
B
ARPE-19
HEK293T
hTERT RPE-1
NIH/3T3
SH-SY5Y
Cilium length (µm)
Serum Starvation (hours): 0 8 16 24 48 72 96
cilia: 15 22 41 22 82 96 55
0 24 48 72
44 39 16 10
0 8 16 24 48 72 96
88 67 68 79 92 93 78
Serum Starvation (hours): 0 8 16 24 48 72 96 0 8 16 24 48 72 96 120 144
cilia: 60 231 148 131 116 97 116 5 13 17 10 4 6 8 7 5

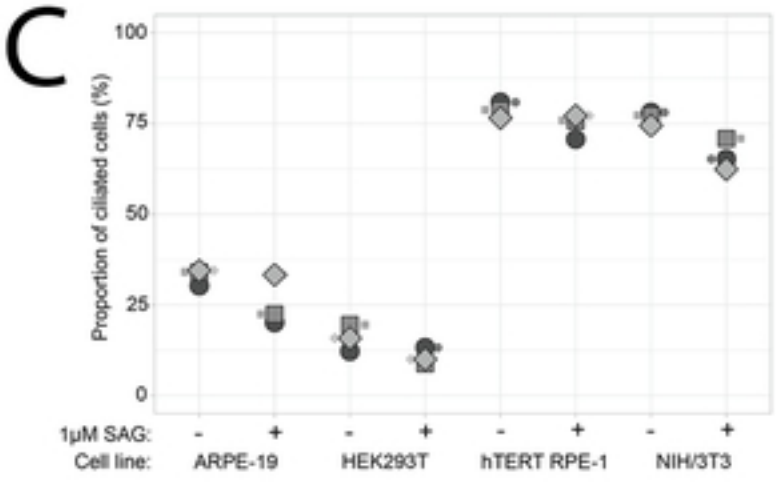
C
Proportion of ciliated cells (%)
1µM SAG: - + - + - + - +
Cell line: ARPE-19 HEK293T hTERT RPE-1 NIH/3T3

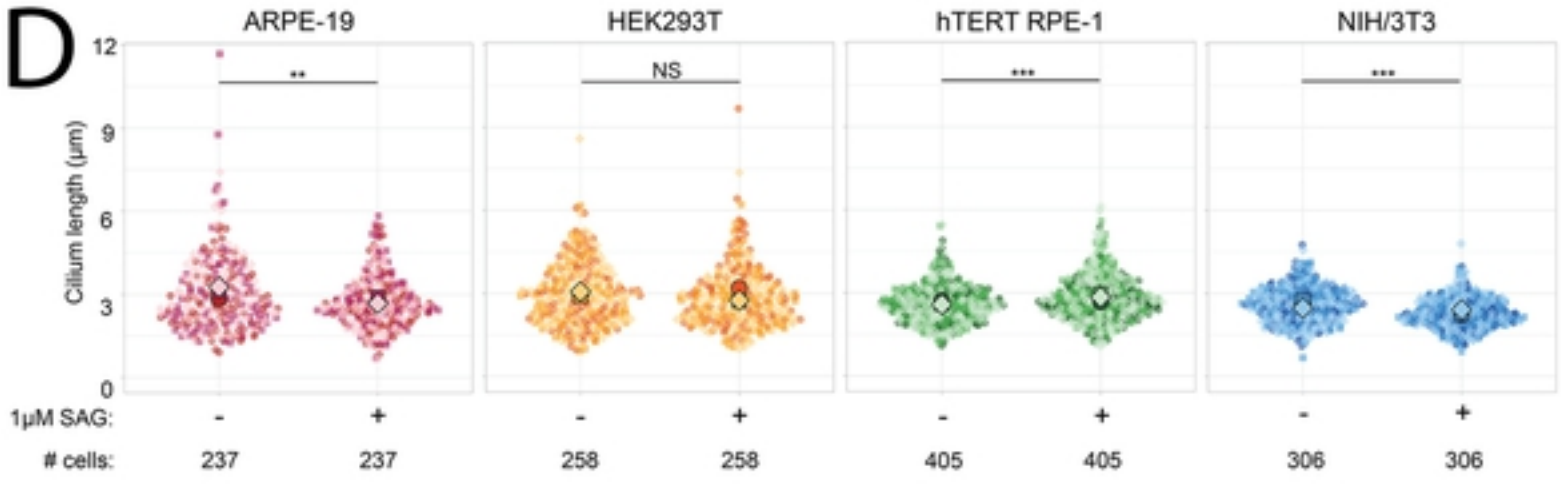
D
ARPE-19
HEK293T
hTERT RPE-1
NIH/3T3
Cilium length (µm)
**
NS
***
***
1µM SAG: - + - + - + - +
cells: 237 237 258 258 405 405 306 306

Figure 1